Electronic Supplementary Material (ESI) for Journal of Materials Chemistry A.

Supporting information

One Dimensional Amorphous Porous Iridium-Ruthenium Oxide for Efficient Acidic Oxygen Evolution Reaction

Lamei Li,[§,a] Zifang Cheng,[§,a] Jiaqi Su,[a] Beibei Song,[a] Hao Yu,[b] Yujin Ji,[*,b] Qi Shao,[*,a] and Jianmei Lu[*,a]

[a] College of Chemistry, Chemical Engineering and Materials Science, Soochow University, Jiangsu, 215123, China. E-mails: qshao@suda.edu.cn; lujm@suda.edu.cn

[b] College of Chemistry, Institute of Functional Nano & Soft Materials (FUNSOM), Soochow University, Jiangsu, 215123, China. E-mails: yjji@suda.edu.cn

§ These authors contributed equally to this work.

This PDF file includes:

Supplementary Figure S1 to S21

Supplementary Table S1

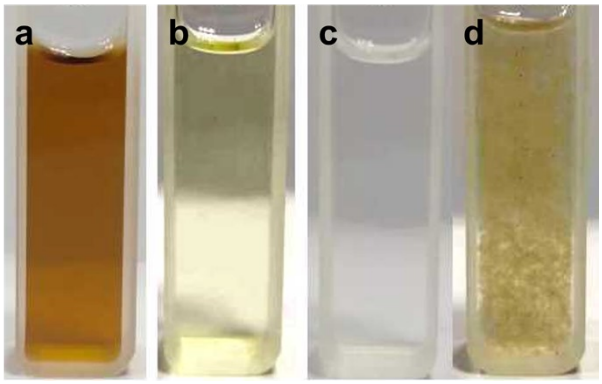

Figure S1. Photographs of reaction mixture at different stages of $SrIr(OH)_6$ NBs synthesis. (a) H_2IrCl_6 aqueous solution, (b) H_2IrCl_6 + KOH mixture before heating, (c) H_2IrCl_6 + KOH mixture after 30 min heating under 70 °C and (d) final products of $SrIr(OH)_6$ NBs after adding $SrCl_2$.

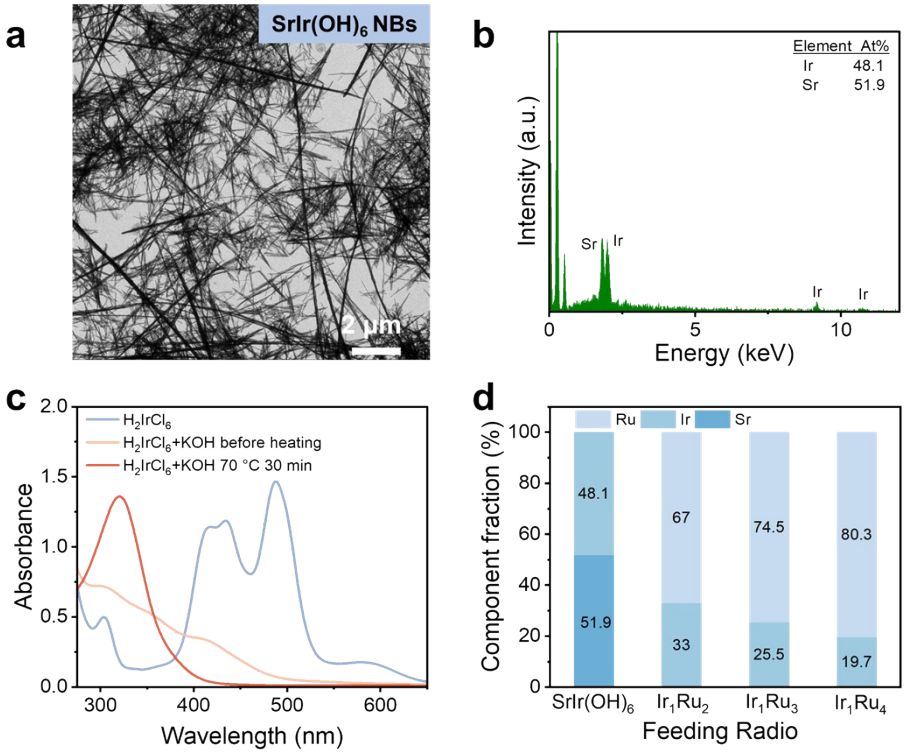

Figure S2. (a) TEM image, (b) SEM-EDS spectra of $SrIr(OH)_6$ NBs, (c) UV-vis spectra of reaction mixtures under different steps and (d) component fractions of different catalysts with different feeding ratios.

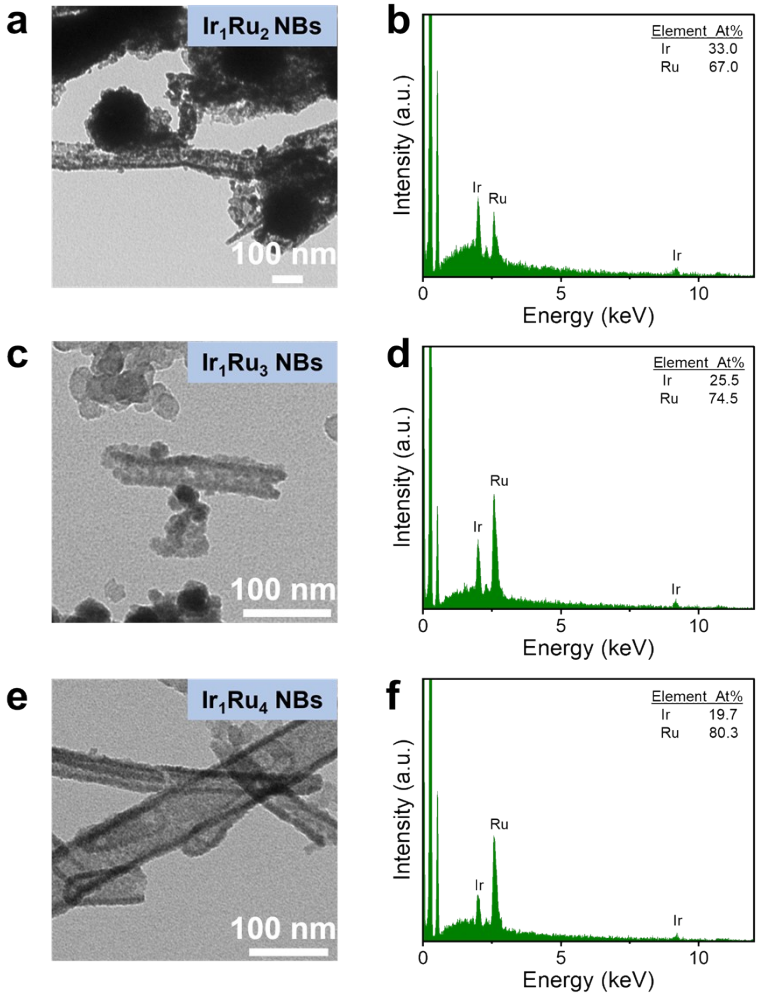

Figure S3. (a, c, e) TEM images and (b, d, f) SEM-EDS spectra of Ir_1Ru_2 NBs, Ir_1Ru_3 NBs and Ir_1Ru_4 NBs.

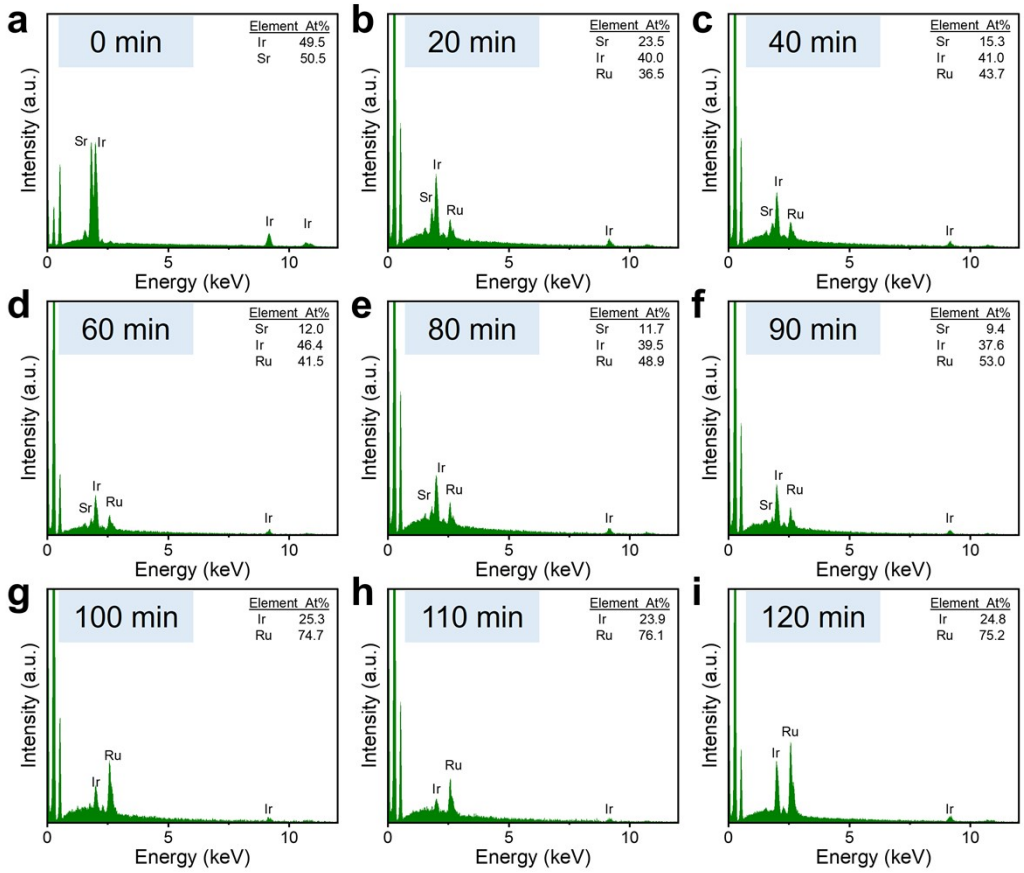

Figure S4. SEM-EDS spectra of Ir_1Ru_3 NBs in the time-tracking experiment at (a) 0 min, (b) 20 min, (c) 40 min, (d) 60 min, (e) 80 min, (f) 90 min, (g) 100 min, (h) 110 min and (i) 120 min.

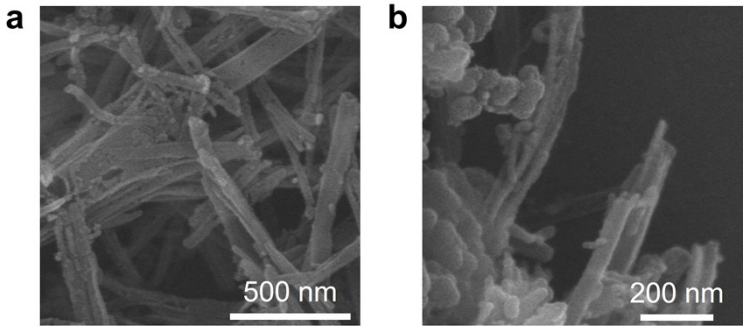

Figure S5. (a, b) SEM images of Am-$Ir_1Ru_3O_8$ NBs-250.

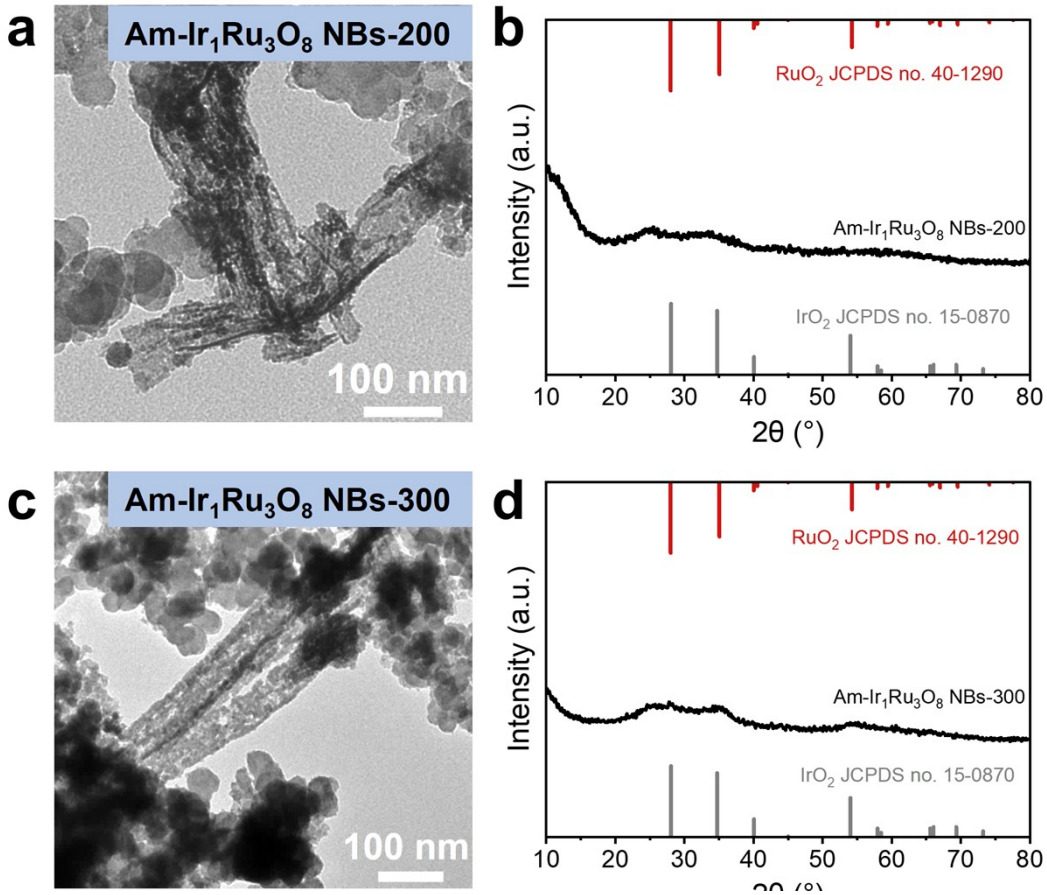

Figure S6. (a, c) TEM images and (b, d) PXRD patterns of Am-$Ir_1Ru_3O_8$ NBs-200 and Am-$Ir_1Ru_3O_8$ NBs-300.

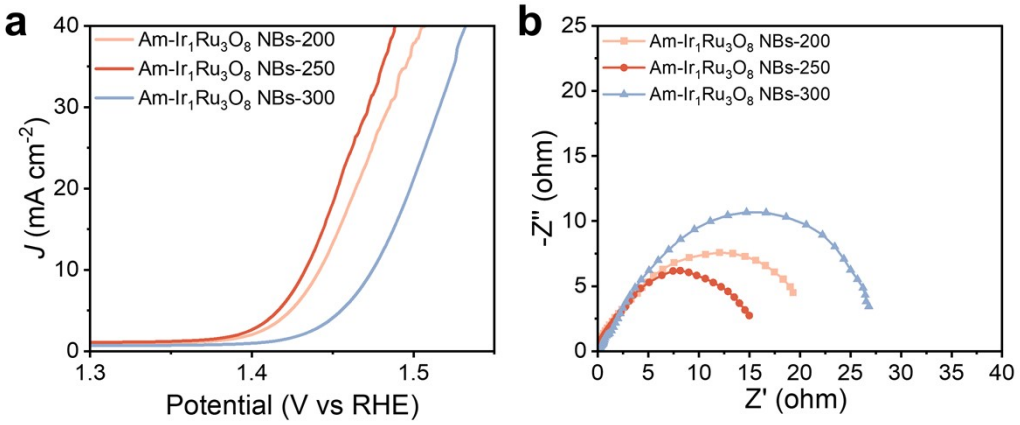

Figure S7. (a) The LSV curves and (b) nyquist plots recorded of Am-$Ir_1Ru_3O_8$ NBs-200, Am-$Ir_1Ru_3O_8$ NBs-250 and Am-$Ir_1Ru_3O_8$ NBs-300.

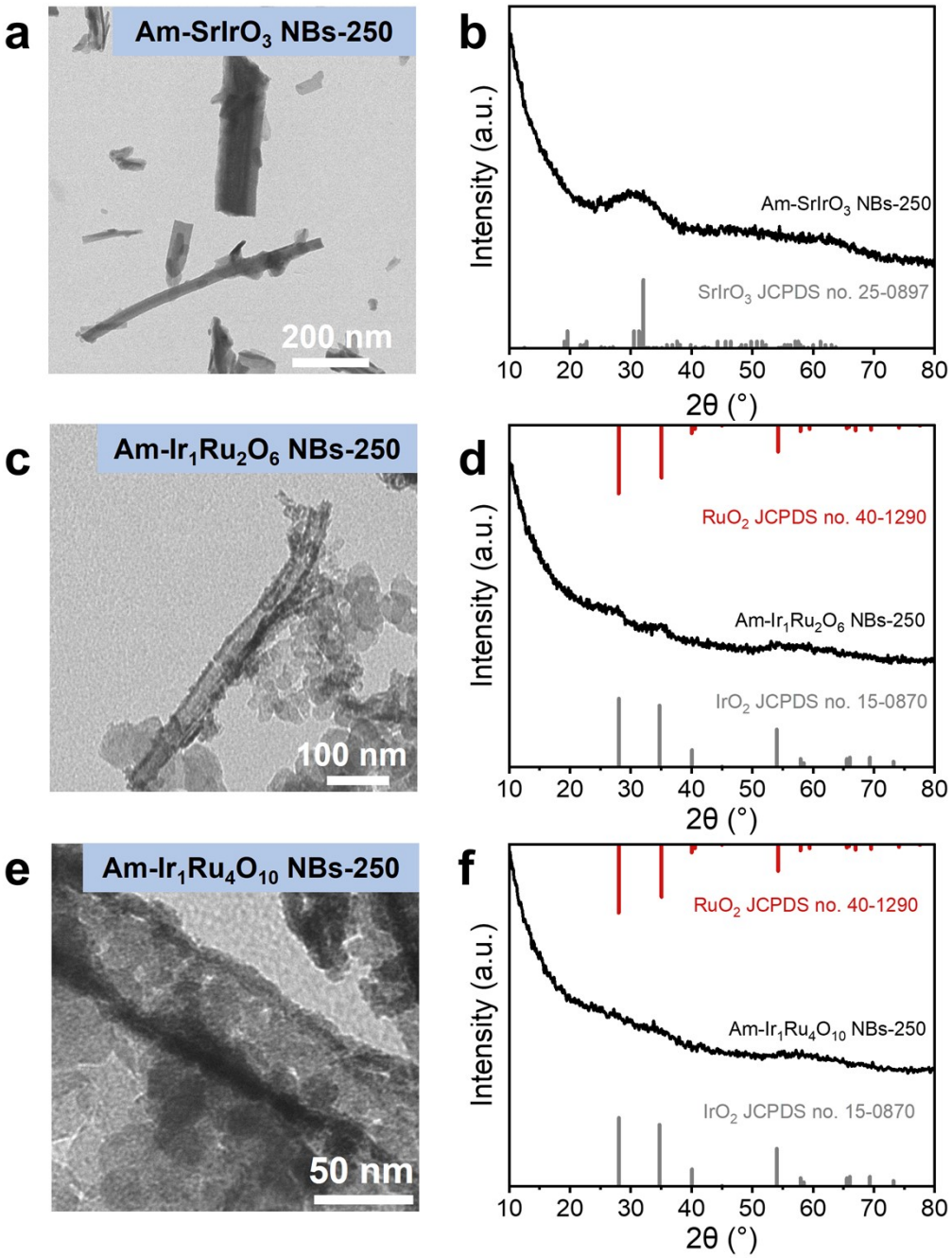

Figure S8. (a, c, e) TEM images and (b, d, f) PXRD patterns of Am-$SrIrO_3$ NBs-250, Am-$Ir_1Ru_2O_6$ NBs-250 and Am-$Ir_1Ru_4O_{10}$ NBs-250.

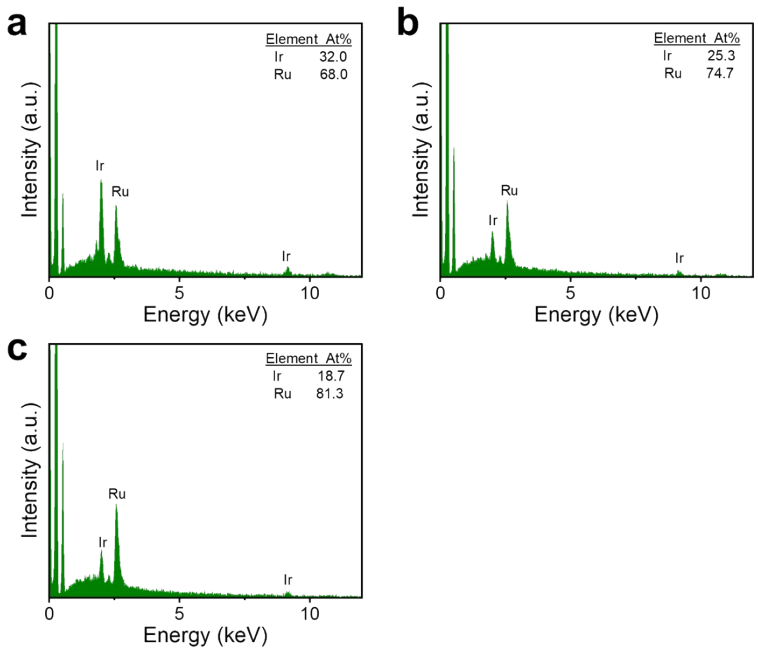

Figure S9. (a, b, c) SEM-EDS spectra of Am-$Ir_1Ru_2O_6$ NBs-250, Am-$Ir_1Ru_3O_8$ NBs-250 and Am-$Ir_1Ru_4O_{10}$ NBs-250.

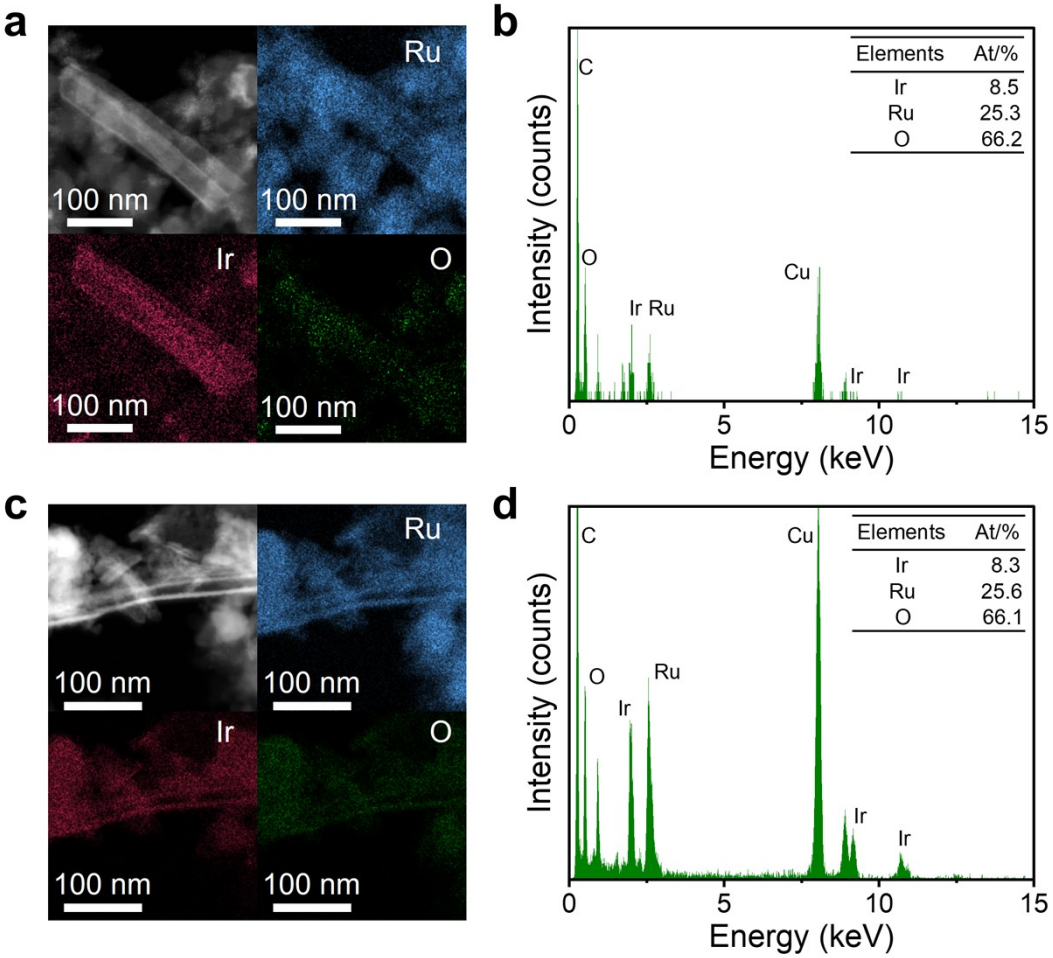

Figure S10. (a, c) HAADF-STEM-EDS mapping and (b, d) HAADF-STEM-EDS of Am-$Ir_1Ru_3O_8$ NBs-250.

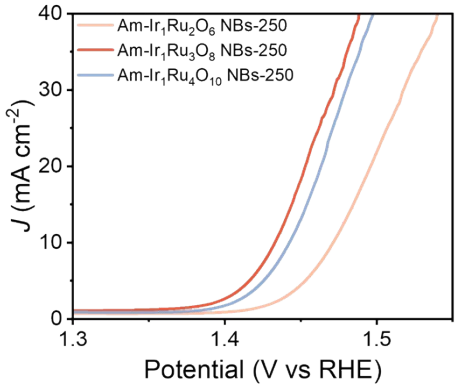

Figure S11. The OER polarization curves of Am-$Ir_1Ru_2O_6$ NBs-250, Am-$Ir_1Ru_3O_8$ NBs-250 and Am-$Ir_1Ru_4O_{10}$ NBs-250.

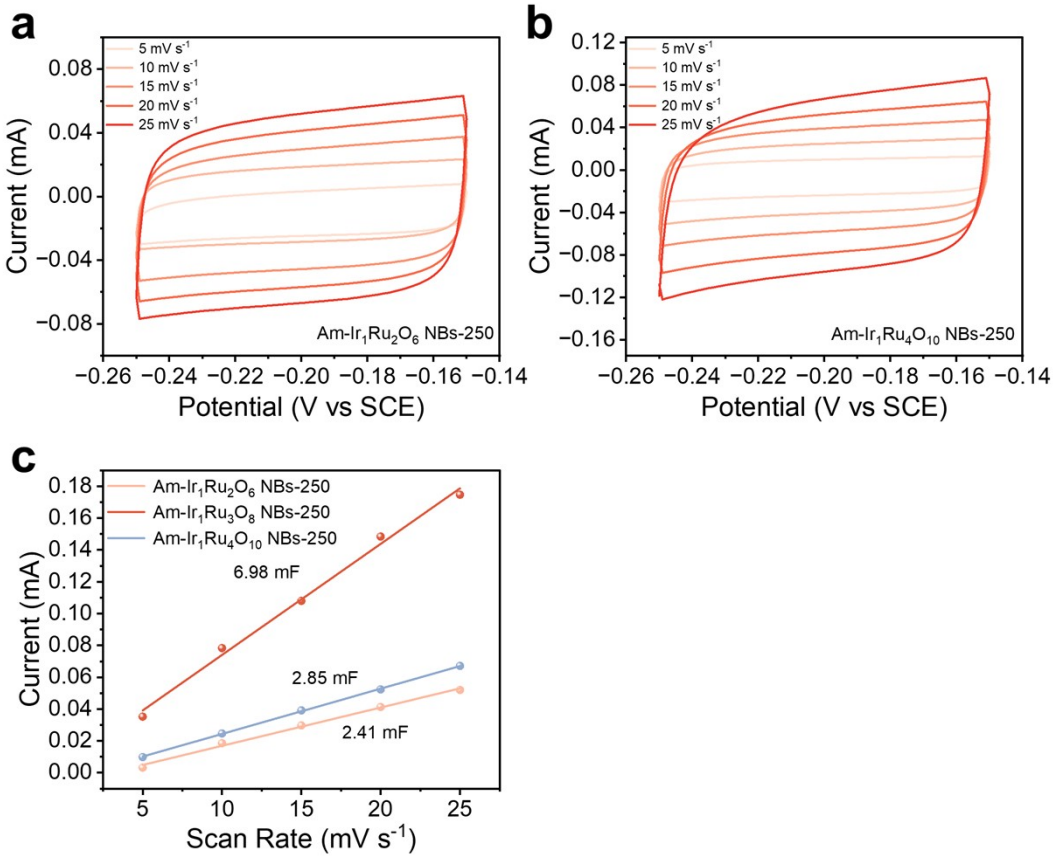

Figure S12. CV curves scanned in the non-faradaic potential window of -0.15 V to -0.25 V at different scan rates for (a) Am-$Ir_1Ru_2O_6$ NBs-250, (b) Am-$Ir_1Ru_4O_{10}$ NBs-250 and (c) charging current plotted against scan rate of Am-$Ir_1Ru_2O_6$ NBs-250, Am-$Ir_1Ru_3O_8$ NBs-250 and Am-$Ir_1Ru_4O_{10}$ NBs-250. The slope of the fitted line represents C_{dl}.

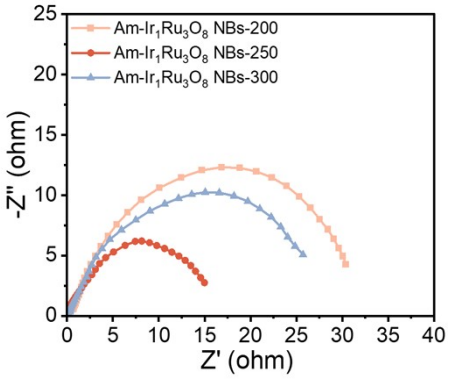

Figure S13. Nyquist plots of Am-$Ir_1Ru_2O_3$ NBs-250, Am-$Ir_1Ru_3O_8$ NBs-250 and Am-$Ir_1Ru_4O_{10}$ NBs-250.

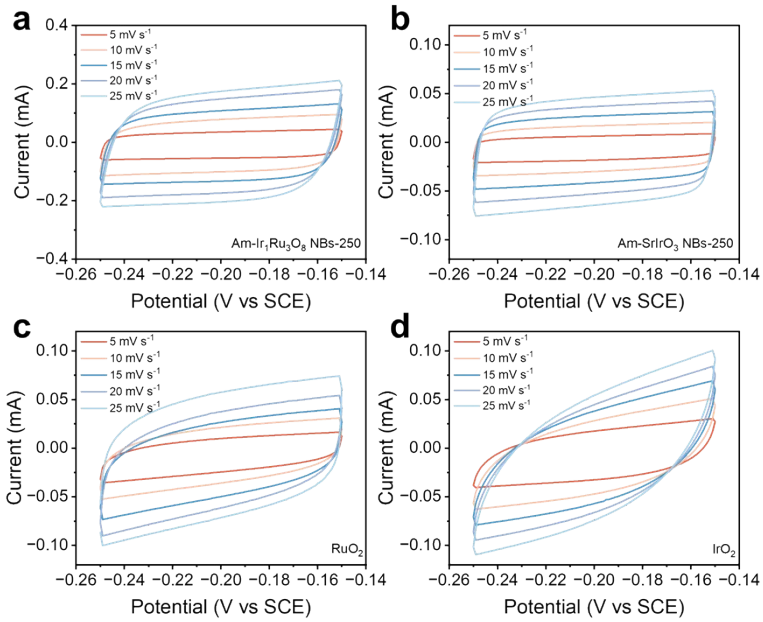

Figure S14. CV curves scanned in the non-faradaic potential window of -0.25 V to -0.15 V at different scan rates for (a) Am-$Ir_1Ru_3O_8$ NBs-250, (b) Am-$SrIrO_3$ NBs-250 and (c) RuO_2 and (d) IrO_2.

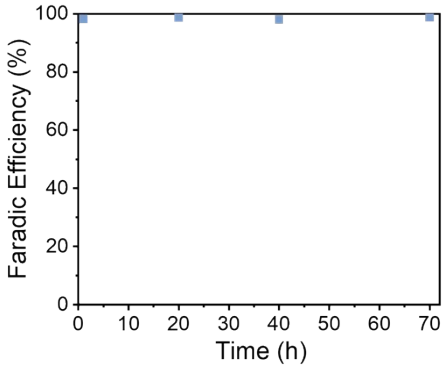

Figure S15. Faraday Efficiency of Am-$Ir_1Ru_3O_8$ NBs-250 during stability test.

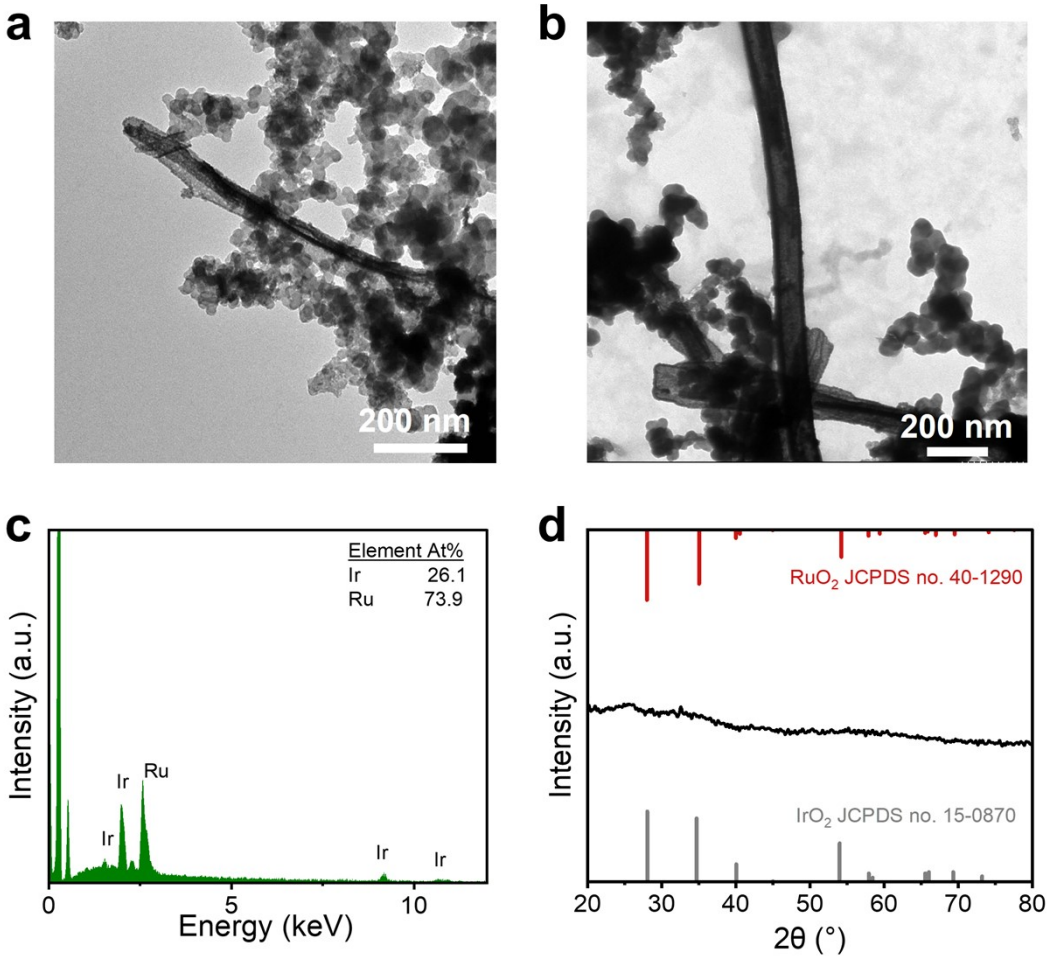

Figure S16. (a) TEM of Am-$Ir_1Ru_3O_8$ NBs-250 before stability test, (b) TEM, (c) SEM-EDS spectra and (d) XRD of Am-$Ir_1Ru_3O_8$ NBs-250 after stability test.

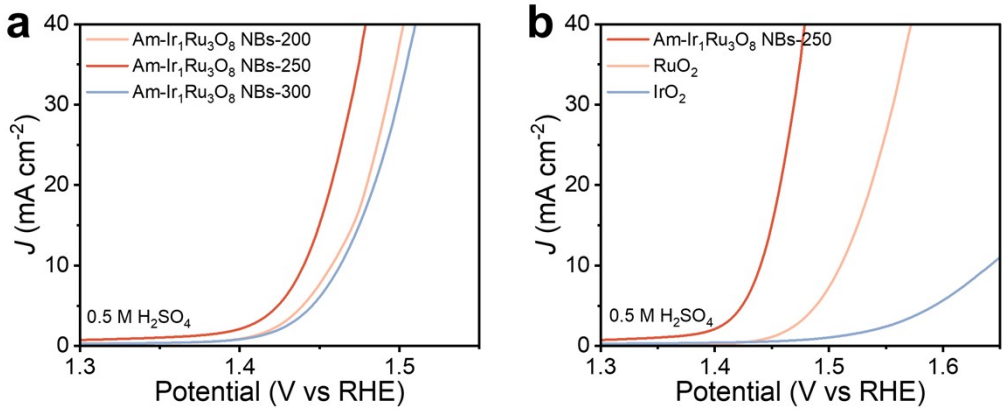

Figure S17. LSV curves of **(a)** Am-$Ir_1Ru_3O_8$ NBs-200, Am-$Ir_1Ru_3O_8$ NBs-250 and Am-$Ir_1Ru_3O_8$ NBs-300 and **(b)** Am-$Ir_1Ru_3O_8$ NBs-200, RuO_2 and IrO_2 in 0.5 M H_2SO_4.

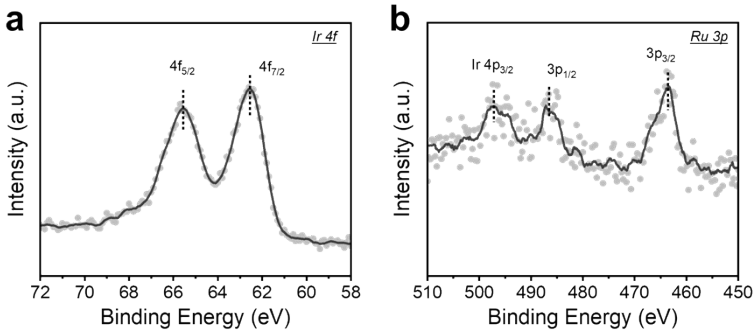

c

	Area Radio(Ir_{4p}/Ru_{3p})
Before stability test	0.24
After stability test	0.4

Figure S18. (a) Ir *4f* , (b) Ru *3p* XPS spectra and (c) the radio of Ir*4p* to Ru*3p* of Am-$Ir_1Ru_3O_8$ NBs-250 after stability test.

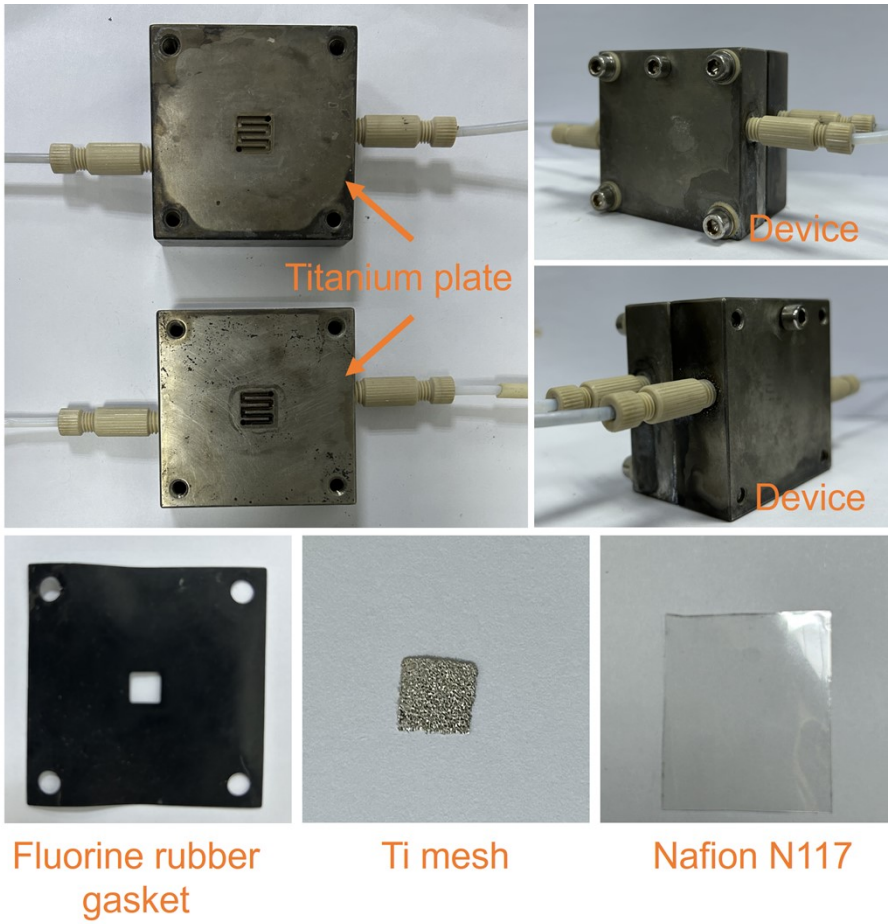

Figure S19. The photograghs of the PEM electrolyzer.

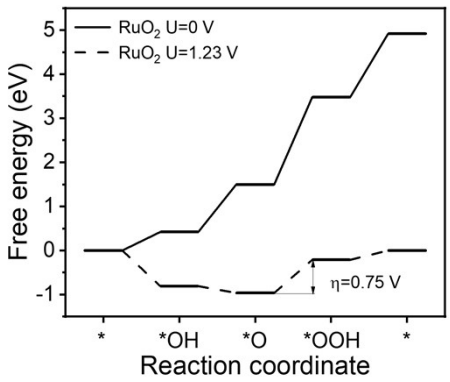

Figure S20. Free energy evolution diagram of four-electron OER on RuO_2 (110) surface.

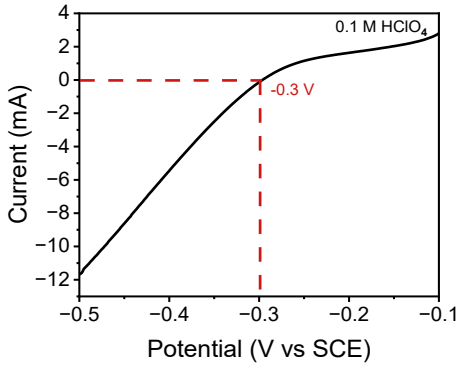

Figure S21. Potential calibration of the saturated calomel electrode (SCE) in 0.1 M $HClO_4$ electrolyte. The calibration of SCE reference electrode is performed in a standard three-electrode system with polished Pt wires as the working and counter electrodes, and the SCE as the reference electrode. Electrolytes are pre-purged and saturated with high purity H_2. Linear scanning voltammetry (LSV) is then run at a scan rate of 5 mV s^{-1}, and the potential at which the current crossed zero is taken to be the thermodynamic potential (vs. SCE) for the hydrogen electrode reactions. For example, in 0.1 M $HClO_4$, the zero current point is at -0.3 V, so E (RHE) = E (SCE) + 0.3 V.

Table S1. Comparison of previous reported Ru or Ir-based catalysts in acidic electrolyte.

Catalyst	Electrolyte	η (mV)	Ref.
Am-$Ir_1Ru_3O_8$ NBs-250	**0.1 M $HClO_4$**	**204 @ 10 mA cm^{-2}**	**This Work**
$Nb_{0.1}Ru_{0.9}O_2$	0.5 M H_2SO_4	204 @ 10 mA cm^{-2}	Joule 2023, 7, 558-573
$Ru_3Ir_1O_x$	0.5 M H_2SO_4	231 @ 10 mA cm^{-2}	Adv. Energy Mater. 2021, 11, 2102883
RuIr-NC	0.05 M H_2SO_4	165 @ 10 mA cm^{-2}	Nat. Commun. 2021, 12, 1145
AD-HN-Ir	0.5 M H_2SO_4	216 @ 10 mA cm^{-2}	Nat. Commun. 2021, 12, 6118
Ni-RuO_2	0.1 M $HClO_4$	214 @ 10 mA cm^{-2}	Nat. Mater. 2023, 22, 100-108
Ru@IrO_X	0.05 M H_2SO_4	282 @ 10 mA cm^{-2}	Chem 2019, 5, 445-459
RuIr	0.5 M H_2SO_4	239 @ 10 mA cm^{-2}	J. Am. Chem. Soc. 2021, 143, 6482-6490
SrRu	0.5 M H_2SO_4	238 @ 10 mA cm^{-2}	J. Am. Chem. Soc. 2021, 143, 6482-6490
Co-RuIr	0.1 M $HClO_4$	235 @ 10 mA cm^{-2}	Adv. Mater. 2019, 31, 1900510
6H-$SrIrO_3$	0.5 M H_2SO_4	248 @ 10 mA cm^{-2}	Nat. Commun. 2018, 9, 5236
RuIr@CoNC	0.5 M H_2SO_4	223 @ 10 mA cm^{-2}	ACS Catal. 2021, 11, 3402-3413
Nano RuO_2	0.5 M H_2SO_4	232 @ 10 mA cm^{-2}	ACS Catal. 2019, 10, 1152-1160
Re-IrO_2	0.5 M H_2SO_4	255 @ 10 mA cm^{-2}	Small 2023, 19, 2207847
AD-HN-Ir	0.5 M H_2SO_4	216 @ 10 mA cm^{-2}	Nat. Commun. 2021, 12, 6118